

**NLO  $\text{QCD}$  Corrections for Higgs Production via VBF  
in Association of Three Jets at the LHC**



Terrance Figy  
Institute for Particle Physics Phenomenology  
Durham University

In Collaboration with D. Zeppenfeld and V. Hankele

## Outline

The NLO Calculation

VBF Cuts

NLO vs LO

Final Remarks

## The NLO Calculation

### The ingredients:

- Born: 3 final state partons + Higgs via VBF

$$\mathcal{M}_B = \delta_{i_2 i_b} t_{i_1 i_a}^{a_3} \left[ \mathcal{M}_{B,1a} : \begin{array}{c} \text{Diagram 1: } a \xrightarrow{\text{wavy}} 1, b \xrightarrow{\text{wavy}} 2, \text{ Higgs } H \text{ (dashed)} \\ \text{Diagram 2: } a \xrightarrow{\text{wavy}} 1, b \xrightarrow{\text{wavy}} 2, \text{ Higgs } H \text{ (dashed)} \end{array} \right] \\ + \delta_{i_1 i_a} t_{i_2 i_b}^{a_3} \left[ \mathcal{M}_{B,2b} : \begin{array}{c} \text{Diagram 1: } a \xrightarrow{\text{wavy}} 1, b \xrightarrow{\text{wavy}} 2, \text{ Higgs } H \text{ (dashed)} \\ \text{Diagram 2: } a \xrightarrow{\text{wavy}} 1, b \xrightarrow{\text{wavy}} 2, \text{ Higgs } H \text{ (dashed)} \end{array} \right]$$

- Virtual:
  - Vertex + Propagator + Box
  - Pentagon + Hexagon
- Real: 4 final state partons + Higgs via VBF

T. M. Figy, Ph.D. Thesis, UMI-32-34582.

### Box+Vertex+Propagator corrections

$$\begin{aligned}
 \text{Box} &= \delta_{i_2 i_b} t_{i_1 i_a}^{a_3} \left[ \text{Box(1a)} : \right. \\
 &\quad \left. \begin{array}{c} \text{Diagram 1a: } a \text{ (solid)} \rightarrow \text{Loop (solid)} \rightarrow 1 \\ \text{Diagram 1a: } b \text{ (solid)} \rightarrow \text{Loop (solid)} \rightarrow 2 \end{array} \right] \\
 &+ \delta_{i_1 i_a} t_{i_2 i_b}^{a_3} \left[ \text{Box(2b)} : \right. \\
 &\quad \left. \begin{array}{c} \text{Diagram 2b: } a \text{ (solid)} \rightarrow \text{Loop (solid)} \rightarrow 1 \\ \text{Diagram 2b: } b \text{ (solid)} \rightarrow \text{Loop (solid)} \rightarrow 2 \end{array} \right]
 \end{aligned}$$

## Hexagons and pentagons

These graphs contribute to the virtual corrections for  $qQ \rightarrow qQgH$  and are color suppressed.

$$\text{Hex(1a)} + \text{Pent(1a)} = \left\{ \begin{array}{c} \text{Diagram 1a: } a \text{ (top), } b \text{ (bottom), } 1 \text{ (right), } 2 \text{ (left). } \\ \text{Diagram 2a: } a \text{ (top), } b \text{ (bottom), } 1 \text{ (right), } 2 \text{ (left). } \\ \text{Diagram 3a: } a \text{ (top), } b \text{ (bottom), } 1 \text{ (right), } 2 \text{ (left). } \\ \text{Diagram 4a: } 1 \text{ (top), } b \text{ (bottom), } a \text{ (right), } 2 \text{ (left). } \\ \text{Diagram 5a: } 1 \text{ (top), } b \text{ (bottom), } a \text{ (right), } 2 \text{ (left). } \\ \text{Diagram 6a: } 1 \text{ (top), } b \text{ (bottom), } a \text{ (right), } 2 \text{ (left). } \\ \text{Diagram 7a: } 1 \text{ (top), } b \text{ (bottom), } a \text{ (right), } 2 \text{ (left). } \\ \text{Diagram 8a: } 1 \text{ (top), } b \text{ (bottom), } a \text{ (right), } 2 \text{ (left). } \\ \text{Diagram 9a: } 1 \text{ (top), } b \text{ (bottom), } a \text{ (right), } 2 \text{ (left). } \\ \text{Diagram 10a: } 1 \text{ (top), } b \text{ (bottom), } a \text{ (right), } 2 \text{ (left). } \\ \text{Diagram 11a: } 1 \text{ (top), } b \text{ (bottom), } a \text{ (right), } 2 \text{ (left). } \end{array} \right\}$$

$$\begin{aligned} 2 \operatorname{Re} [\mathcal{M}_V \mathcal{M}_B^*] &= d_F^2 C_F^2 2 \operatorname{Re} [(\text{Box(1a)}) \mathcal{M}_{B,1a}^*] \\ &+ d_F^2 C_F^2 2 \operatorname{Re} [(\text{Box(2b)}) \mathcal{M}_{B,2b}^*] \\ &+ \frac{d_F^2 C_F^2}{d_G} 2 \operatorname{Re} [(\text{Hex(1a)} + \text{Pent(1a)}) \mathcal{M}_{B,2b}^*] \\ &+ \frac{d_F^2 C_F^2}{d_G} 2 \operatorname{Re} [(\text{Hex(2b)} + \text{Pent(2b)}) \mathcal{M}_{B,1a}^*] \end{aligned}$$

To a first approximation, we may neglect the contribution of the hexagons and pentagons.

## Consistent treatment of the Real Corrections

$$\mathcal{M}_4(1_q, 2_Q, 3_g, 4_g, a_q, b_Q) = \left\{ \begin{array}{c} \text{Feynman diagrams for } \mathcal{M}_4 \end{array} \right. + \dots \left. \right\}$$

$$|\mathcal{M}_4|^2 = d_F^2 C_F^2 \left\{ \left| \begin{array}{c} \text{Diagram 1} \end{array} \right|^2 + \left| \begin{array}{c} \text{Diagram 2} \end{array} \right|^2 + \left| \begin{array}{c} \text{Diagram 3} \end{array} \right|^2 + \left| \begin{array}{c} \text{Diagram 4} \end{array} \right|^2 + \dots \right\} \\ + \frac{d_F^2 C_F^2}{d_G} 2 \operatorname{Re} \left\{ \left( \begin{array}{c} \text{Diagram 1} \end{array} \right) \left( \begin{array}{c} \text{Diagram 2} \end{array} \right)^* + \left( \begin{array}{c} \text{Diagram 3} \end{array} \right) \left( \begin{array}{c} \text{Diagram 4} \end{array} \right)^* + \dots \right\}$$

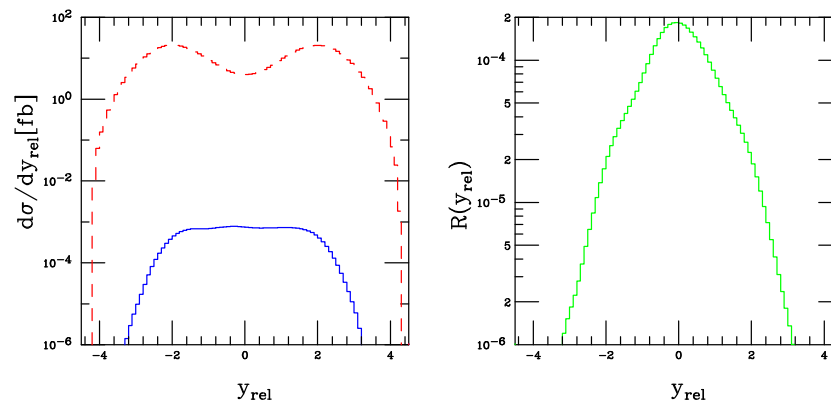
The term  $\propto 1/d_G$  when integrated over PS gives rises to a soft divergence. This soft divergence is cancelled against the soft divergence arising from the hexagons and pentagons. **For consistency, this term is also neglected.**

## Error Estimate on the Approximation

$$\Delta\text{NLO} \propto 2 \operatorname{Re} \left[ \left( \mathcal{M}_{B,1a} : \begin{array}{c} 3 \\ \text{---} \\ a \xrightarrow{\quad} 1 \\ | \\ \text{---} \\ b \xrightarrow{\quad} 2 \\ H \end{array} + \dots \right) \left( \mathcal{M}_{B,2b} : \begin{array}{c} 1 \\ \text{---} \\ a \xrightarrow{\quad} \\ | \\ \text{---} \\ b \xrightarrow{\quad} 2 \\ H \\ 3 \end{array} + \dots \right)^* \right]$$

Left:  $\Delta\sigma_3^{NLO}$  (solid) and  $\sigma_3^{LO}$  (dashes).

Right:  $R(y_{\text{rel}}) = \Delta\text{NLO}/\text{LO}$



$\Delta\sigma_3^{NLO} \approx 10^{-3} \text{ fb}$  for VBF cuts in the CJV region with  $m_h = 120 \text{ GeV}$ .

## NLO parton level Monte Carlo Program

- The dipole subtraction method of Catani and Seymour is used to regulate the IR divergences of the real emission corrections [hep-ph/9605323].
- Have introduced a cut,  $\alpha$ , on the PS of the dipoles as a consistency check [hep-ph/0307268].
- Born amplitudes are calculated numerically using the helicity amplitude formalism.
- Real amplitudes were generated using MADGRAPH.
- Identical particle effects have been neglected.
- $b$ -quarks have been included for neutral current processes.
- The Monte Carlo integration is performed with a modified form of VEGAS.
- CTEQ6M PDFs are used at NLO with  $\alpha_s(M_Z) = 0.118$  while CTEQ6L1 PDFs are used at LO with  $\alpha_s(M_Z) = 0.130$ .
- SM parameters are computed using LO electroweak relations with  $M_Z$ ,  $M_W$ , and  $G_F$  as inputs.
- Jets are reconstructed from final-state partons by the use of the  $k_T$  algorithm with  $D = 0.8$ .

## VBF Cuts

- $k_T$  algorithm: Require at least 3 hard jets with  $p_{Tj} \geq 20$  GeV and  $|y_j| \leq 4.5$ .
- Tagging jets: 2 jets of  $p_{Tj}^{\text{tag}} \geq 30$  GeV and  $|y_j^{\text{tag}}| \leq 4.5$ .
- Higgs decay products:

$$p_{T\ell} \geq 20 \text{ GeV}, \quad |\eta_\ell| \leq 2.5, \quad \Delta R_{j\ell} \geq 0.6 \quad (1)$$

$$y_{j,\min}^{\text{tag}} + 0.6 < \eta_{\ell_{1,2}} < y_{j,\max}^{\text{tag}} - 0.6. \quad (2)$$

- Rapidity gap and opposite detector hemispheres:

$$y_j^{\text{tag } 1} \cdot y_j^{\text{tag } 2} < 0 \quad (3)$$

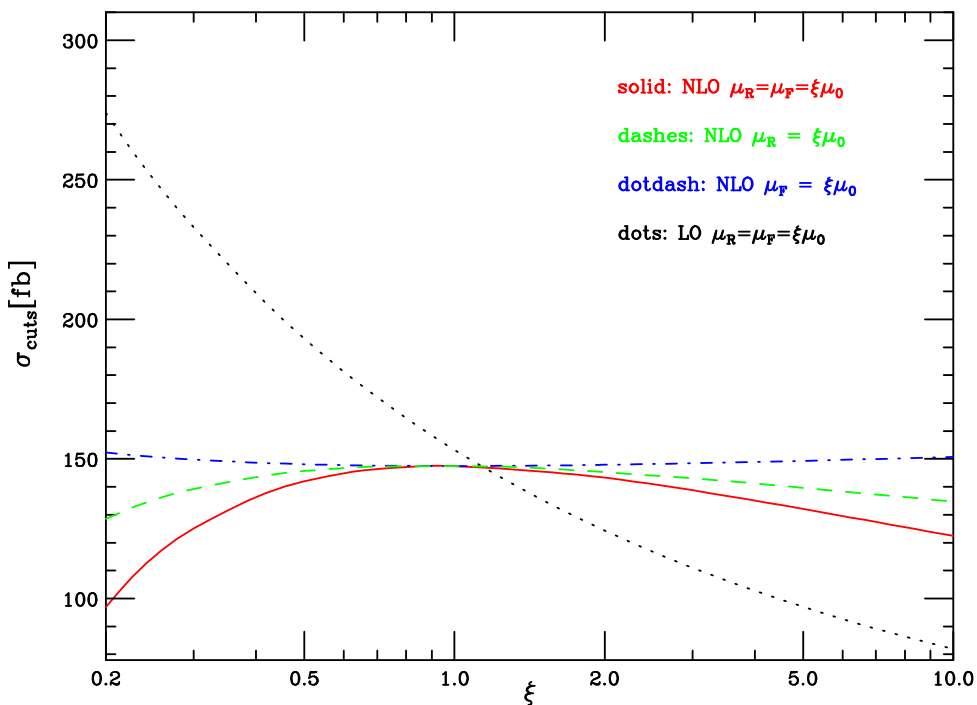
$$\Delta y_{jj} = |y_j^{\text{tag } 1} - y_j^{\text{tag } 2}| > 4 \quad (4)$$

- Invariant mass of tagging jets:

$$m_{jj} > 600 \text{ GeV} \quad (5)$$

## NLO vs LO

### Total Cross Section at the LHC

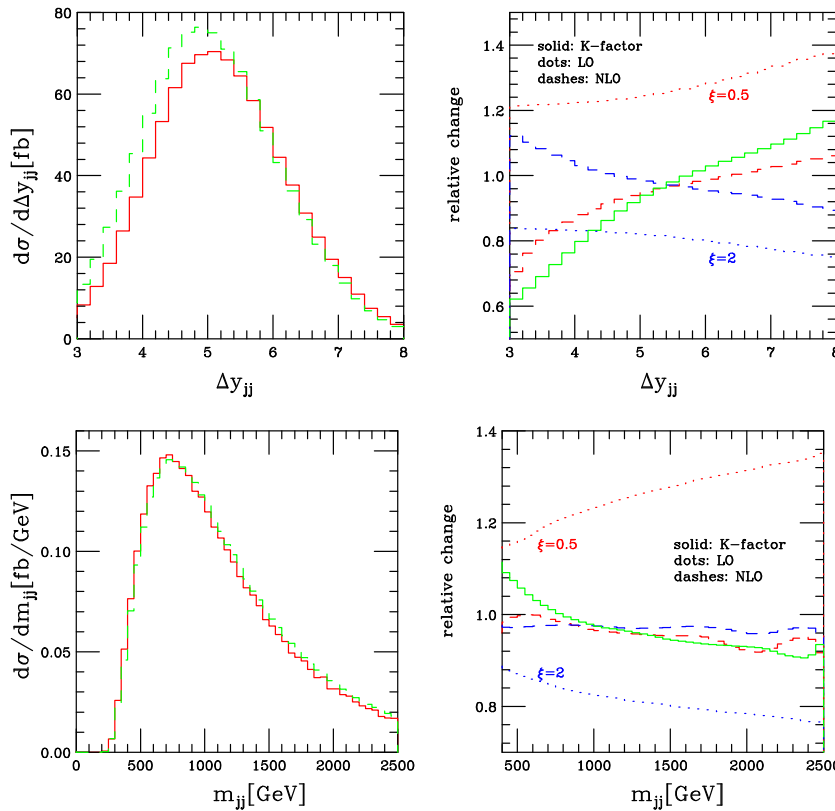


$\mu_0 = 40 \text{ GeV}$   
 $\xi = 2^{\pm 1}$  scale variations:  

- LO: +26% to -19%
- NLO: less than 5%

## NLO vs LO

### Tagging Jet Distributions



Left panel: NLO (solid) and LO (dashed).

Right panel:

$$K(x) = \frac{d\sigma_3^{NLO}(\mu_R = \mu_F = \xi\mu_0)/dx}{d\sigma_3^{LO}(\mu_R = \mu_F = \mu_0)/dx}$$

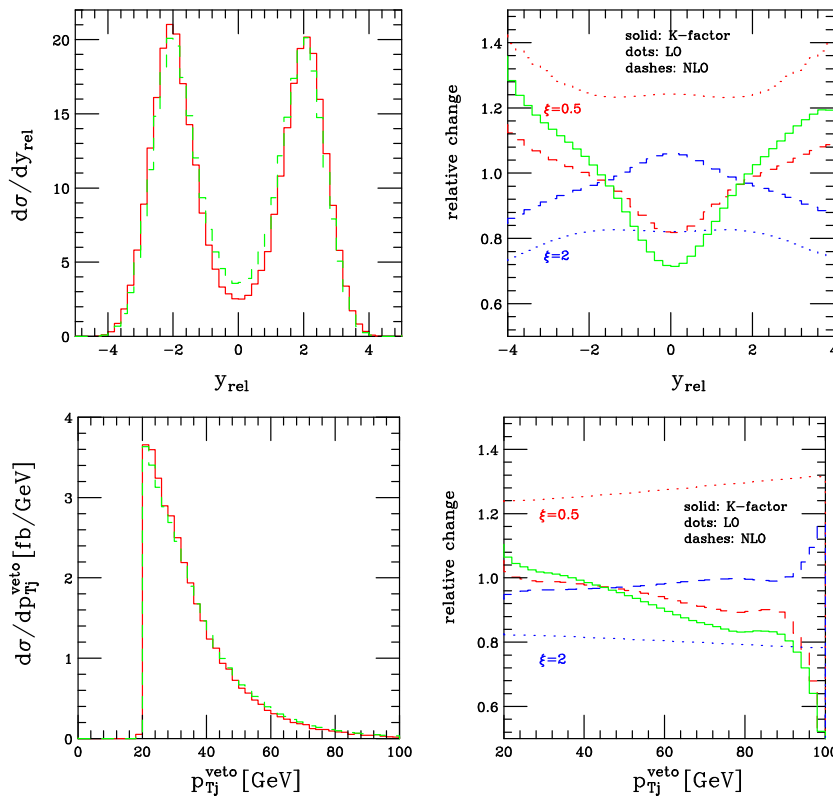
(solid) and

$$\text{relative change} = \frac{d\sigma_3(\mu_R = \mu_F = \xi\mu_0)/dx}{d\sigma_3(\mu_R = \mu_F = \mu_0)/dx}$$

at LO (dots) and NLO (dashes) for  $\xi = 0.5$  and  $\xi = 2$ .

## NLO vs LO

### Veto Jet Distributions



Central Jet Veto (CJV) cuts:

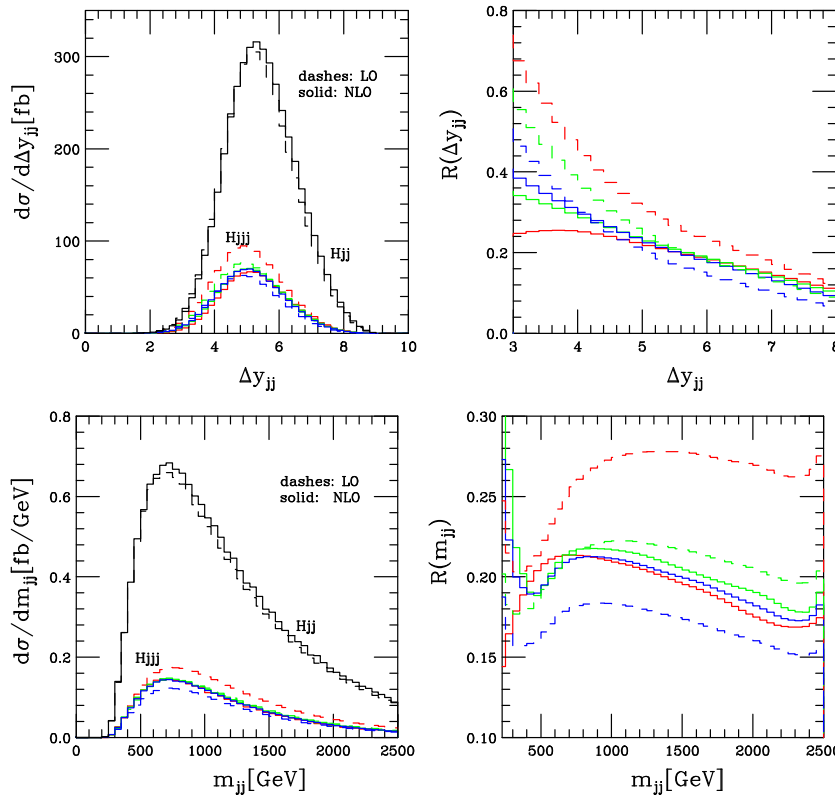
$$p_{Tj}^{\text{veto}} > 20 \text{ GeV}, \quad y_j^{\text{veto}} \in (y_j^{\text{tag } 1}, y_j^{\text{tag } 2}). \quad (6)$$

$$y_{\text{rel}} = y_j^{\text{veto}} - (y_j^{\text{tag } 1} + y_j^{\text{tag } 2})/2$$

- Veto is slightly softer at NLO.
- $\xi = 2^{\pm 1}$  scale variations at  $y_{\text{rel}}=0$ :
  - LO:  $-27\%$  to  $+42\%$
  - NLO:  $-20\%$  to  $+7\%$
- Suppressed radiation in the vicinity of  $y_{\text{rel}} = 0$ .

## NLO vs LO

### VBF H+3 jets vs VBF H+2 jets



Top: VBF cuts, no  $\Delta y_{jj} > 4$ .

Bottom: VBF cuts, no  $m_{jj} > 600$  GeV.

Right panel:

$$R(x) = \frac{d\sigma_3(\mu_R, \mu_F)/dx}{d\sigma_2^{NLO}(\mu_R = \mu_F = m_h)/dx}$$

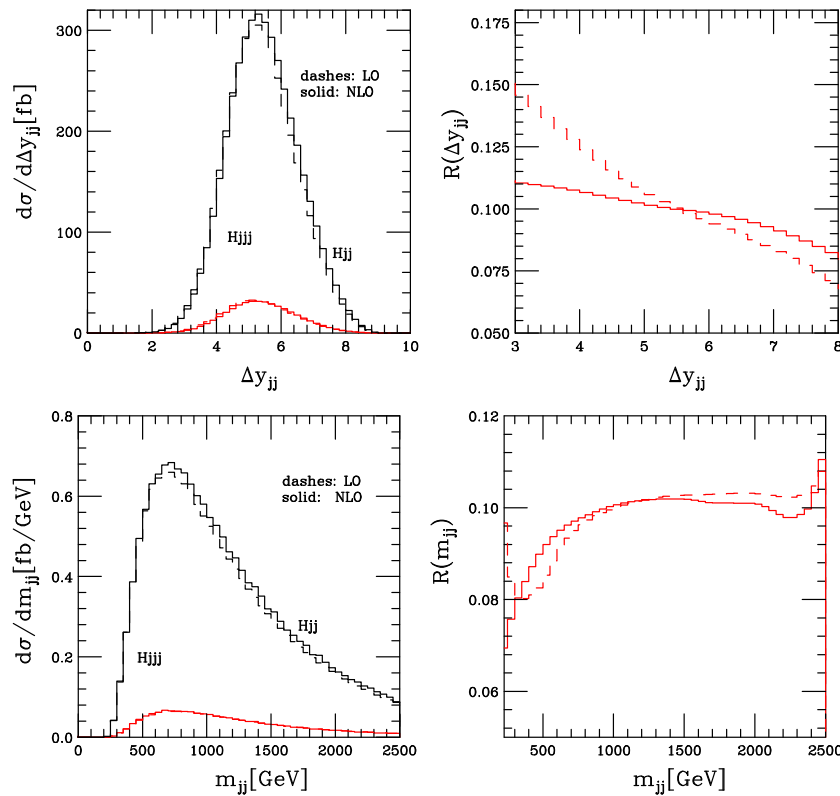
Left panel:

- VBF H+3 jets at NLO (solid colored) and LO (dashes colored) with  $\mu_R = \mu_F = 20, 40, 80$  GeV.
- VBF H+2 jets at NLO (solid black) and LO (dashes black).

T. Figy, C. Oleari and D. Zeppenfeld, Phys. Rev. D **68**, 073005 (2003)

## NLO vs LO

### VBF H+3 jets vs VBF H+2 jets in the CJV region



Top: CJV and VBF cuts, no  $\Delta y_{jj} > 4$ .  
Bottom: CJV and VBF cuts, no  $m_{jj} > 600$  GeV.

Right panel:

$$R(x) = \frac{d\sigma_3(\mu_R, \mu_F)/dx}{d\sigma_2^{NLO}(\mu_R = \mu_F = m_h)/dx}$$

Left panel:

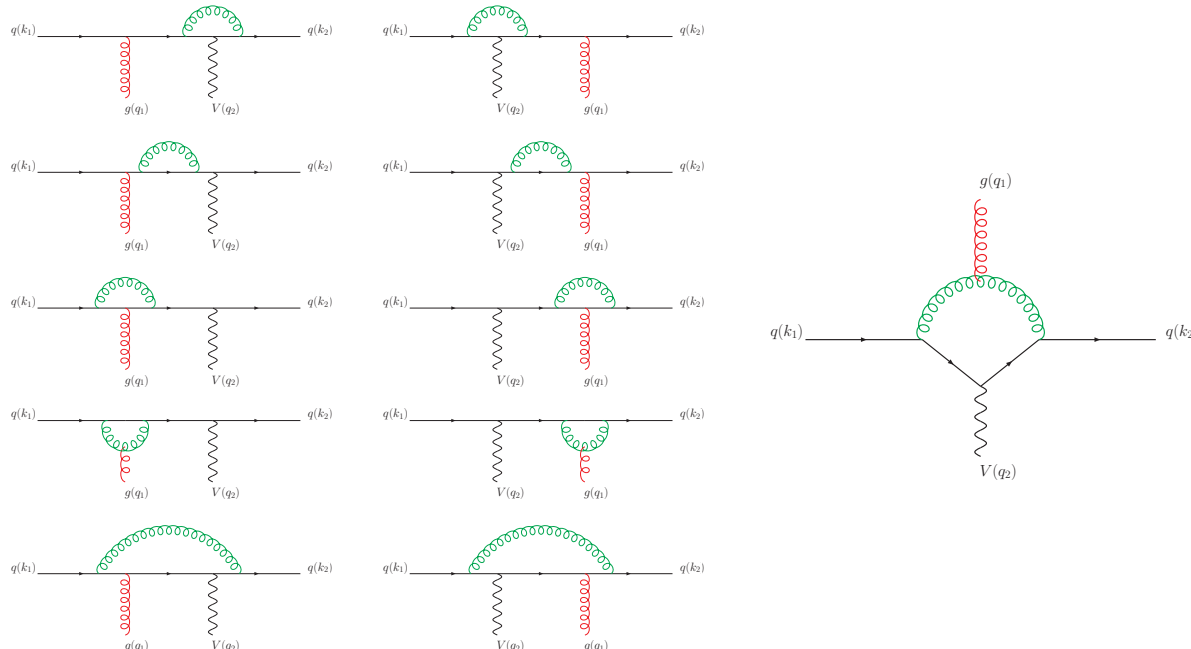
- VBF H+3 jets at NLO (solid) and LO (dashes) with  $\mu_R = \mu_F = 40$  GeV.
- VBF H+2 jets at NLO (solid black) and LO (dashes black).

## Final Remarks

- The dominant NLO QCD corrections have been computed for VBF  $Hjjj$  in the form of a fully flexible NLO partonic Monte Carlo program.
- Scale dependence is reduced for the total cross section and distributions at NLO.
- QCD corrections are small.
- $K$  factors are phase space dependent.
- Central radiation is more suppressed at NLO than at LO.

## Box+Propagator+Vertex graphs

PV reduction used to reduce tensor loop integrals to scalar loop integrals.



## Real emission graphs

